

Influence of the alkyl substitution position on photovoltaic properties of 2D-BDT-based conjugated polymers

Huifeng Yao, Long Ye, Benhu Fan, Lijun Huo* and Jianhui Hou*

Three conjugated polymers based on thienyl-substituted benzodithiophene (BDT) and 4,7-bis-thienyl-benzothiadiazole (DTBT) with varied substitution positions of the alkyl side chains were synthesized to investigate the correlations between the structure and photovoltaic performance of the polymer photovoltaic materials. The three polymers named PBDTDTBT-*p*, PBDTDTBT-*o* and PBDTDTBT-*m* were characterized by a set of methods including absorption spectroscopy, cyclic voltammetry, thermogravimetric analysis, X-ray diffraction, density functional theory and photovoltaic measurements. The results show that the steric hindrance caused by the different substitution positions of the alkyl chains has a significant influence on the photovoltaic properties of the polymers. The open-circuit voltage (V_{oc}) of the photovoltaic devices based on the three polymers could range from 0.67 to 0.90 V. Clearly, this finding provides us a feasible strategy to optimize the photovoltaic properties by simply changing the positions of the alkyl chains.

INTRODUCTION

Design, synthesis and applications of novel conjugated polymers for polymer solar cells (PSCs) have received substantial attention over the past decades [1–14]. Significant improvements have been achieved in understanding the correlations between polymer structure and photovoltaic performance, which have helped to boost the power conversion efficiency (PCE) over 7% in several well-known backbones, such as benzodithiophene (BDT) and thienothiophene (TT) (PBDT-TT) [15–28], BDT and benzothiadiazole (BT) (PBDT-BT) [29,30], BDT and thienopyrrole-dione (TPD) (PBDT-TPD) [31], etc.

Besides the extensive studies on design of new backbone structures, side chain engineering is emerging as an important strategy to optimize the structure of photovoltaic polymers [32–34]. Generally, researchers focus on the length (namely, carbon atom number) and type (straight or branched) of alkyl chains, which all affect the performance of the photovoltaic polymers. Based on the previous studies, several requirements should be considered for high

performance polymers. First, alkyl side chain should afford the solubility of the rigid conjugated polymers toward good film-forming property. Second, alkyl side chain could also tune the optical absorption, molecular energy levels and morphologies of the photovoltaic materials. For instance, a dramatic improvement was obtained in PBDT-TPD based PSCs through a simple tuning of the side chain length, and a high PCE up to 8.5% was achieved by Cabanetos and co-workers [31]. However, compared with aforementioned cases, only a very few of studies took considerations of the substitution position effect of alkyl chains in studies of photovoltaic polymers [35–37]. Therefore, to investigate the effect of substitution positions of the alkyl chains should be of great importance for structure optimization of photovoltaic polymers, and this will provide guidance for designing high performance photovoltaic materials.

Previously, we developed an efficient copolymer based on thienyl-substituted BDT and 4,7-di (thiophen-2-yl) benzothiadiazole (DTBT) units, which exhibited a high open-circuit voltage (V_{oc}) of ~0.9 V and a PCE over 5% [38]. In the present work, in order to get more insights into the impact of alkyl chain substitution positions on photovoltaic properties of the PBDTDTBT polymers [38,39], a long branched para-hexyldecyl, two ortho-dioctyl and two meta-dioctyl side chains were introduced onto the thiophene group in varied positions, respectively. Then three copolymers named PBDTDTBT-*o*, PBDTDTBT-*m* and PBDTDTBT-*p* were synthesized (see Scheme 1), and the systematical study revealed the effects of the alkyl chain positions on absorption spectra, molecular energy levels, crystallinities, morphological and photovoltaic properties of the PBDTDTBT polymers.

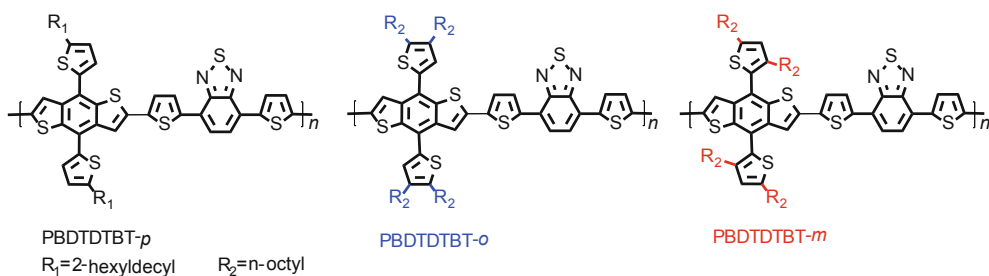
RESULTS AND DISCUSSION

Synthesis of the polymers

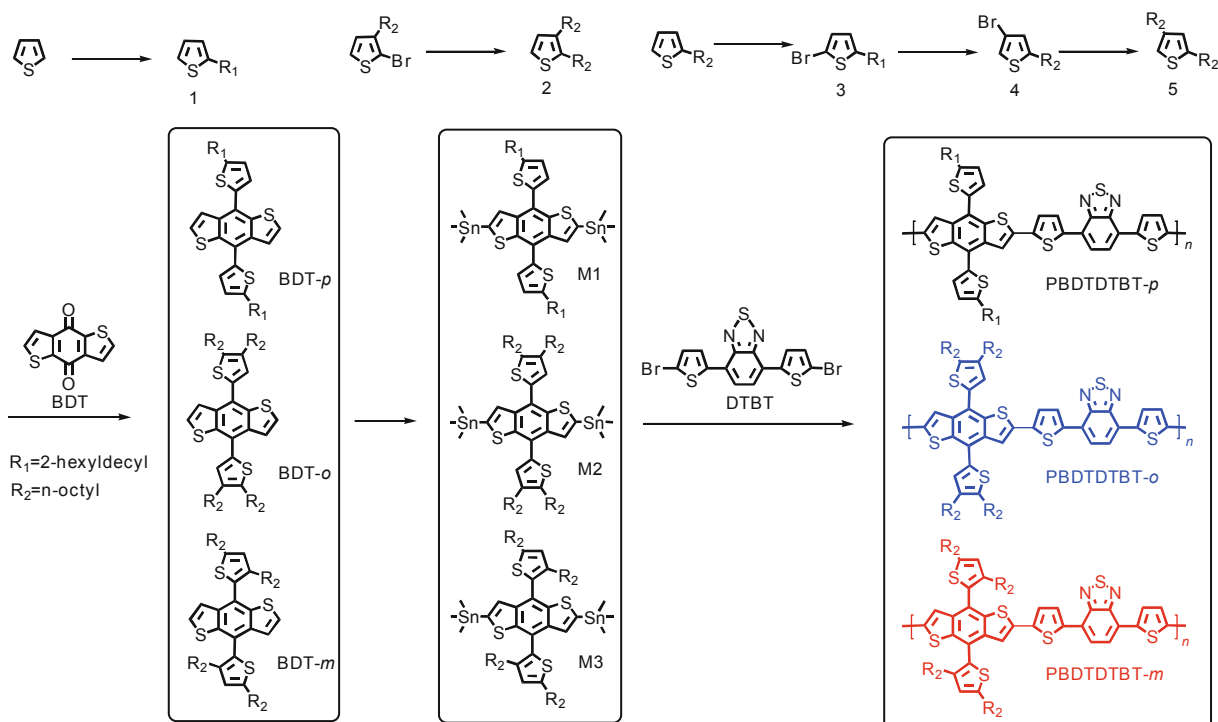
The synthetic routes of the three copolymers are described

State Key Laboratory of Polymer Physics and Chemistry, Beijing National Laboratory for Molecular Sciences, Institute of Chemistry, Chinese Academy of Sciences, Beijing, 100190, P. R. China

* Corresponding authors (emails: hjhzl@iccas.ac.cn (Hou J); huolijun@iccas.ac.cn (Huo L))



Scheme 1 Molecular structures of PBDDTDTBT based polymers with varied alkyl side chain positions.



Scheme 2 Synthetic routes of the three kinds of polymers.

in Scheme 2. The thiophene derivatives with different alkyl chains were synthesized and introduced onto BDT units by the same method as reported in our previous work [38], after which the monomers were obtained from the reaction with trimethyltin chloride. The three polymers were prepared through Stille coupling reaction. More synthetic details are given in the Experiment Section. The number average molecular weights (M_n) of PBDDTDTBT-*p*, PBDDTDTBT-*o*, PBDDTDTBT-*m* are 28 k Da (polydispersities (PDI) = 1.9), 25 k Da (PDI = 1.7) and 18 k Da (PDI = 1.8), respectively. The thermal stability of the three polymers were studied by thermogravimetric analysis (TGA), and the TGA plots of these polymers are shown in Fig. 1. It can be seen that the decomposition temperatures (T_d) at 5%

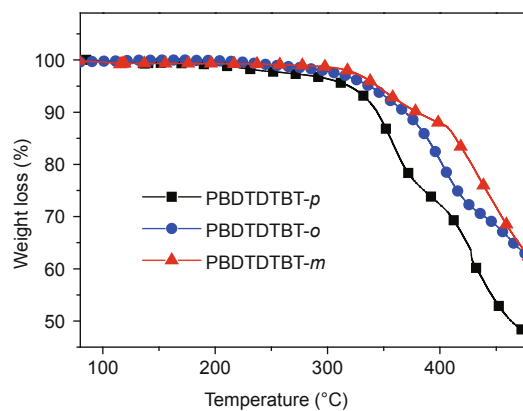


Figure 1 TGA plots of the polymers under the protection of nitrogen with a heating rate of 10 °C min⁻¹.

weight loss are all above 300°C for the three polymers.

Optical properties

The UV-vis absorption spectra of the three polymers in chloroform and solid thin films are shown in Fig. 2, and the detailed parameters are listed in Table 1. From Fig. 2a, it can be observed that three absorption bands of these polymers and the corresponding absorption peaks of the three polymers locate at 613, 593 and 579 nm for PBDTDTBT-*p*, PBDTDTBT-*o* and PBDTDTBT-*m* respectively. The optical band gaps calculated according to the absorption edges of the polymer films are listed in Table 1. Interestingly, comparing the absorption spectra of the polymers in solution with that in films from the Fig. 2b, the onset points of the absorption of PBDTDTBT-*p* and PBDTDTBT-*o* are almost overlapped in solution while 14 nm red-shift is observed from PBDTDTBT-*o* to PBDTDTBT-*p* in thin films. This phenomenon suggests stronger intermolecular π - π

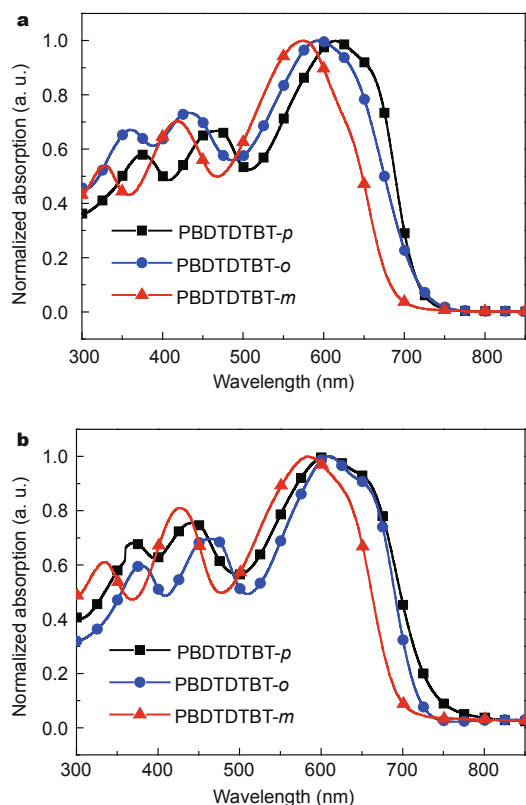


Figure 2 Normalized UV-vis absorption spectra of the three polymers: (a) in chloroform solution, and (b) thin films on quartz.

Table 1 Optical and electrochemical properties of the polymers

Polymer	λ_{\max} (nm)	λ_{\max} (nm)	E_g^{opt} (eV)	HOMO (eV)	$\mu_{\text{hole}} \text{ cm}^2 \text{ V}^{-1} \text{ s}^{-1}$
	Solution	Film			
PBDTDTBT- <i>p</i>	613	607	1.64	-5.09	3.50×10^{-3}
PBDTDTBT- <i>o</i>	593	613	1.68	-5.11	8.61×10^{-3}
PBDTDTBT- <i>m</i>	579	596	1.75	-5.31	9.26×10^{-4}

interaction may be formed in the PBDTDTBT-*p* film than in PBDTDTBT-*o* film, which indicates that two ortho-position substituted alky side chains possess stronger steric hindrance than one para-position substituted alkyls.

Electrochemical properties

Electrochemical cyclic voltammetry (CV) was used to measure the molecular energy levels of the three polymers. As shown in Fig. 3, all the three polymers show reversible *p*-doping processes. The oxidation potential of PBDTDTBT-*p* is 0.29 V. PBDTDTBT-*o* shows a little higher oxidation potential (0.31 V) than PBDTDTBT-*p* by 0.02 V. It is obvious that the oxidation potential of PBDTDTBT-*m* is (0.51 V) ca. 0.2 V higher than those of the other two polymers. The highest occupied molecular orbital (HOMO) levels of these polymers were calculated according to the equation: $\text{HOMO} = -e(\phi_{\text{ox}} + 4.80)$ (eV), and the detailed data are listed in Table 1.

Computational study

In order to further explore the effect of alkyl chain positions on the molecular energy levels and molecular conformations of the polymers, theoretical calculation was performed by using density functional theory (DFT) with the B3LYP/6-31G** basis set (Gaussian 09 [40]). With the purpose of reducing the cost of calculation, only the alkyl substituted BDTs were employed and the long alkyl chains were replaced by $-\text{CH}_2\text{CH}_3$ group. The calculated molecular geometries and the frontier molecular orbitals are collected in Table 2.

The calculated HOMO levels of BDT-*p*, BDT-*o*, BDT-*m* change from -5.11, -5.16 to -5.26 eV, and the trend is quite consistent with the results of corresponding polymers from CV tests. The electron density distributions of BDT-*p*, BDT-*o* have little difference, i.e., the π -electrons can be delocalized onto both the BDT units and the substituted thio-

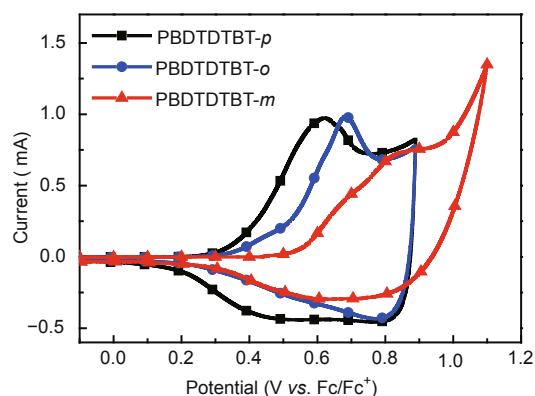
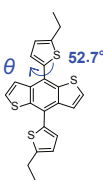
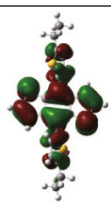
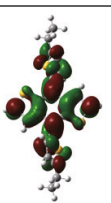
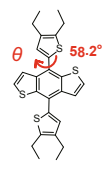
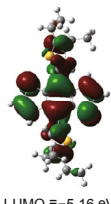
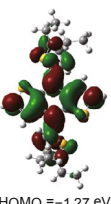
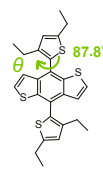
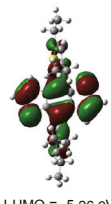
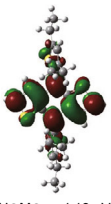


Figure 3 Cyclic voltammogram plots of the polymers on glassy carbon electrode in 0.1 mol L⁻¹ Bu₄NPF₆ in acetonitrile solution at a scan rate of 50 mV s⁻¹.

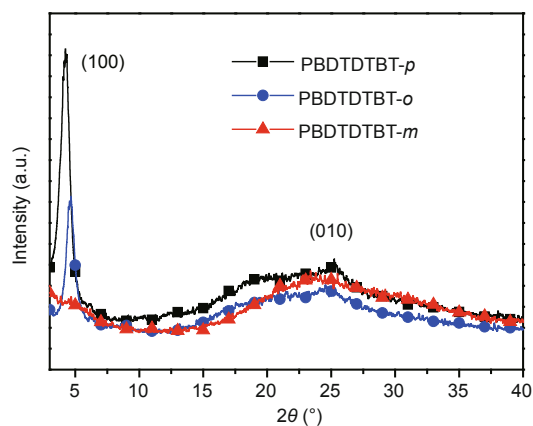
Table 2 Calculated HOMO and lowest unoccupied molecular orbital (LUMO) electron density distributions of the alkyl substituted BDTs

BDTs	Conformation	HOMO	LUMO
BDT- <i>p</i>		 HOMO = -5.11 eV	 LUMO = -1.30 eV
BDT- <i>o</i>		 LUMO = -5.16 eV	 HOMO = -1.27 eV
BDT- <i>m</i>		 LUMO = -5.26 eV	 HOMO = -1.19 eV

phene units. However the π -electron of BDT-*m* is mainly localized on the BDT unit. It should be noted that the dihedral angles (θ) between the thiophene and BDT units change a lot when the alkyls are introduced onto different positions, i.e., the dihedral angles are 52.7°, 58.2° and 87.8° for BDT-*p*, BDT-*o* and BDT-*m*, respectively. These results indicate that the steric hindrance is increased gradually from BDT-*p* to BDT-*o* and then to BDT-*m*, which is probably the origin of the variations of the absorption spectra and electrochemical results.

X-ray diffraction (XRD) analysis

XRD was used to examine the crystalline structure of the polymers in thin film. As shown in Fig. 4, for PBDDTDTBT-*p* and PBDDTDTBT-*o*, diffraction signals in (100) direction at 4.26° (corresponding to a *d*-spacing of 20.72 Å) and 4.70° (a *d*-spacing of 18.78 Å) are observed distinctly. The increased distance of lamellar spacing from PBDDTDTBT-*o* to PBDDTDTBT-*p* may be caused by the longer alkyl chain of 2-hexyldecyl than octyl. For PBDDTDTBT-*m* film, no clear diffraction peak can be observed in this region, which means PBDDTDTBT-*m* has less ordered arrangement in this direction. The polymers of PBDDTDTBT-*p*, PBDDTDTBT-*o* and PBDDTDTBT-*m* exhibit weak but clear diffraction signals in the direction of (010) at 25.36°, 24.57° and 23.31°, respectively, corresponding to π - π stacking distances of 3.52, 3.61 and 3.81 Å. The intensity of (100) reflection peaks

**Figure 4** X-ray diffraction patterns of three polymers films casted from chloroform.

decreased a lot from PBDDTDTBT-*p* and PBDDTDTBT-*o* to PBDDTDTBT-*m*. The larger π - π stacking distance and weaker lamellar reflection indicate that PBDDTDTBT-*p* possesses the most orderly arrangement while PBDDTDTBT-*m* has the worst. Moreover, the results are consistent with the phenomenon observed in the absorption spectra and the theoretical calculation.

Hole mobility

Hole mobilities of the blend films based on the three PBDDT-

DTBT polymers were measured by using space-charge-limited current (SCLC) method and the results are listed in Table 1. In the SCLC measurement, a device configuration of indiumtin oxide (ITO)/poly(3,4-ethylenedioxythiophene):poly(styrenesulfonate)(PEDOT:PSS)/polymer:PC₇₁BM/Au(80 nm) and the optimal processing conditions in PSC devices were used. The hole mobilities of PBDTDTBT-*p*, PBDTDTBT-*o* and PBDTDTBT-*m* were calculated as 3.50×10^{-3} , 8.61×10^{-3} and $9.26 \times 10^{-4} \text{ cm}^2 \text{ V}^{-1} \text{ s}^{-1}$, respectively (Fig. 5).

Photovoltaic behaviors

PSCs with a device structure of ITO/PEDOT:PSS/ polymer: PC₇₁BM/Ca (20 nm) /Al (100 nm) were fabricated to investigate the photovoltaic properties of the polymers, and the donor/acceptor (D/A) weight ratios were optimized by using dichlorobenzene (DCB) as the processing solvent. In order to acquire the optimal performances of these devices, thermal annealing was also carried out. *J-V* characteristics are shown in Fig. 6 and the corresponding results are summarized in Table 3.

The open-circuit voltage (V_{oc}) values of the optimal devices fabricated based on PBDTDTBT-*p*, PBDTDTBT-*o* and PBDTDTBT-*m* are quite different, changing from 0.67,

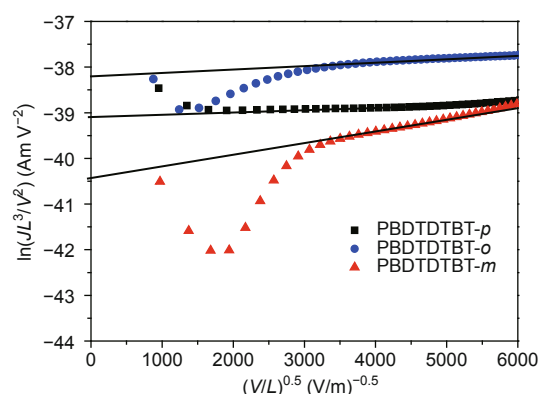


Figure 5 $\ln(JL^3/V^2)$ versus $(VL)^{0.5}$ plots of the polymer:PC₇₁BM blends for the SCLC measurements.

0.75 to 0.90 V, which are highly dependent to their different HOMO levels. For PSC devices based on PBDTDTBT-*p*, a best PCE of 3.48% with a low V_{oc} of 0.67 V was obtained under a D/A ratio of 1:1 after thermal annealing at 110°C for 10 minutes. The processing condition of PBDTDTBT-*o* was the same with that of PBDTDTBT-*p*. A higher V_{oc} of 0.75 V with a better PCE of 5.76% was achieved in the devices based on PBDTDTBT-*o*. The devices of PBDTDTBT-*m* shows the highest V_{oc} of 0.90 V, and the optimal

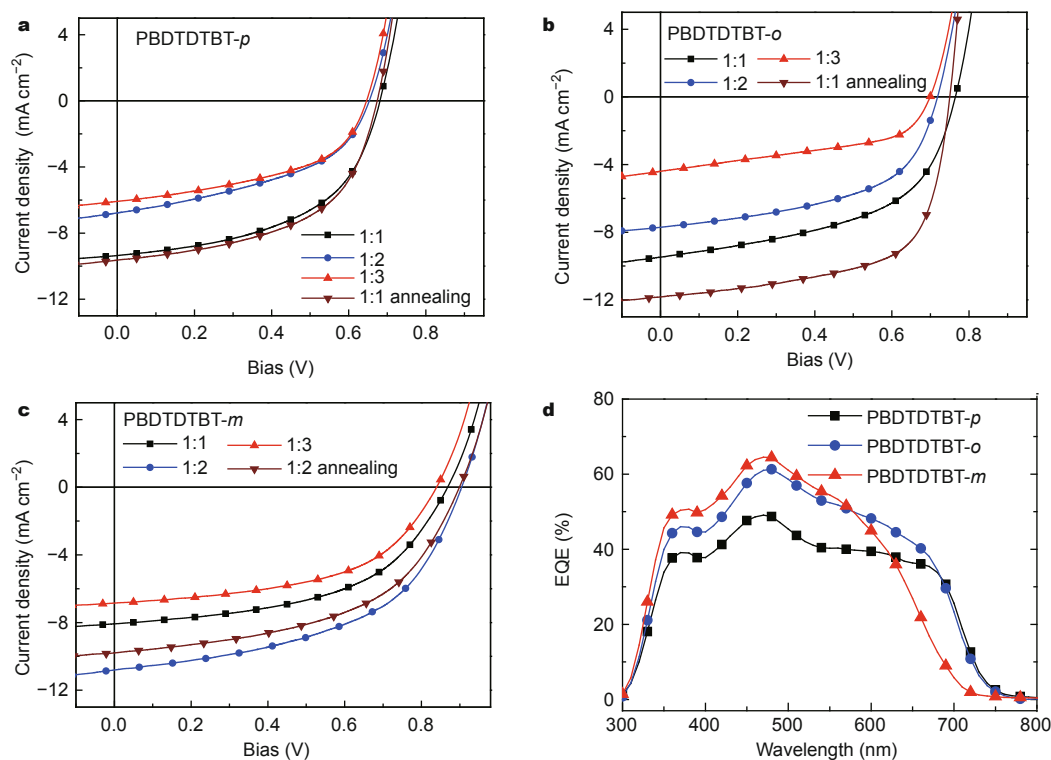


Figure 6 *J-V* curves of the devices based on polymers/PC₇₁BM with different donor/acceptor ratios and annealing condition under illumination of AM 1.5G, 100 mW cm^{-2} : (a) PBDTDTBT-*p*, (b) PBDTDTBT-*o*, (c) PBDTDTBT-*m*; (d) the external quantum efficiency (EQE) curves of the PSCs devices fabricated by the optimal conditions.

Table 3 Photovoltaic parameters of the PSCs based on the PBDTDTBT/PC₇₁BM

Polymer	Weight ratio	V_{oc} (V)	J_{sc} (mA cm ⁻²)	FF (%)	PCE (%)	Thickness (nm)
PBDTDTBT- <i>p</i>	1:1	0.68	9.35	51	3.25	–
	1:2	0.65	6.77	45	2.00	–
	1:3	0.65	6.08	49	1.92	–
	1:1 ^a	0.67	9.63	54	3.48	95
PBDTDTBT- <i>o</i>	1:1	0.76	9.47	52	3.78	–
	1:2	0.72	7.71	53	2.94	–
	1:3	0.70	3.96	49	1.37	–
	1:1 ^a	0.75	11.82	65	5.76	105
PBDTDTBT- <i>m</i>	1:1	0.87	8.07	51	3.61	–
	1:2	0.90	10.81	53	5.16	98
	1:3	0.85	6.85	57	3.32	–
	1:2 ^a	0.90	9.79	55	4.85	–

a) thermal annealing at 110°C for 10 min

D/A weight ratio was 1:2. Compared with the other polymers, the J_{sc} decreased slightly after thermal annealing in the PBDTDTBT-*m* case, so a PCE of 5.16% with the highest V_{oc} of 0.90 V was obtained from the condition without post-treatment. The active layer thicknesses of the optimal PSC devices were around 95–105 nm.

Morphology

The morphologies of the blend films based on the three polymers were studied by atomic force microscopy (AFM). Fig. 7 shows the AFM height images of the three blend films coated by the optimal conditions. The root mean square (RMS) roughness values of PBDTDTBT-*p*:PC₇₁BM, PBDTDTBT-*o*:PC₇₁BM are 3.48 and 2.21 nm respectively, while PBDTDTBT-*m* has a higher RMS of 5.11 nm. The random arrangement of PBDTDTBT-*m* may result in a relatively higher RMS when the polymer chains stack to each other. The discrepancy in morphology should be connected to the difference in J_{sc} values of the devices and consequently affects the overall efficiency.

CONCLUSION

In summary, to get a comprehensive insight into the impact of alkyl substitution positions on photovoltaic properties

of the 2D-BDT-based polymers, three polymers named PBDTDTBT-*p*, PBDTDTBT-*o*, PBDTDTBT-*m* with the identical conjugated backbone were designed and synthesized. Due to the different steric hindrance caused by the substitution positions, these polymers exhibit different optical and electrical properties, and also the molecular packing and surface morphologies of these polymer films are also very different. In detail, PBDTDTBT-*o* and PBDTDTBT-*p* show little difference in optical band gaps and energy levels for their relative small discrepancy in steric hindrance, while PBDTDTBT-*m* exhibits the largest band gap and the deepest HOMO level among these polymers, due to the strongest steric hindrance caused by the alkyl side groups. From the analysis of XRD measurements, more ordered inter-molecular arrangement can be found in the films of PBDTDTBT-*p* and PBDTDTBT-*o* than the PBDTDTBT-*m* film. Interestingly, the V_{oc} values of the devices based on these three polymers varied from 0.67, 0.75 to 0.90 V, which should be related to the varied HOMO levels of the polymers. Overall, the results in this work show that the fine-tuning of substitution positions of the alkyl side groups plays an important role in modulating photovoltaic properties in 2D-BDT-based polymers.

EXPERIMENTAL SECTION

Materials and synthesis

Compound 1, BDT-*p* and M1 were synthesized through our previous method [41]. Pd(PPh₃)₄ and Ni(dppp)Cl₂ were purchased from Frontiers Scientific Inc. The monomer DTBT and PC₇₁BM were purchased from Solarmer Materials Inc. Tetrahydrofuran (THF) was dried over Na/benzophenone and freshly distilled prior to use. All of the other commercial available reagents and compounds were

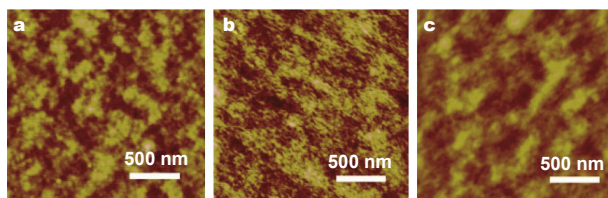


Figure 7 AFM height images (2×2 μm²) of polymer: PC₇₁BM blend films fabricated by the optimal conditions: (a) PBDTDTBT-*p*, (b) PBDTDTBT-*o*, (c) PBDTDTBT-*m*.

used as received.

Instruments

^1H NMR spectra were performed on a Bruker arx-400 spectrometer in CDCl_3 at room temperature. Absorption spectra were measured on a Hitachi U-3100 UV-vis spectrophotometer. Molecular weights and PDI of the polymers were estimated by gel permeation chromatography (GPC) method using polystyrene as standard and chloroform as eluent. The CHI650D Electrochemical Workstation with Glassy carbon, Platinum wire, and Ag/Ag^+ electrode was used to measure the electrochemical potentials of the polymer films, and the measurement was carried out in a 0.1 M tetrabutylammonium hexafluorophosphate (Bu_4NPF_6) acetonitrile solution. EQE was measured by a Solar Cell Spectral Response Measurement System QE-R3011 (Enli Technology). The light intensity at each wavelength was calibrated with a standard single-crystal Si photovoltaic cell.

Fabrication of polymer solar cells

pSC devices were fabricated with a typical structure of ITO/PEDOT:PSS/polymer:PC₇₁BM/Ca/Al under the following conditions: after spin-coating a 35 nm of PEDOT:PSS onto a pre-cleaned ITO glass substrate, the ITO was dried at 150°C for 15 min. Then the polymer/PC₇₁BM (10 mg mL⁻¹, based on the polymer weight concentration) blend solutions in *o*-dichlorobenzene was spin-coated. Then, methanol treatment (~60 μL methanol was deposited of active layers at 4000 rpm for 30 s) was carried out to improve the reproducibility and efficiency of all of the PSC devices for realizing better interface contacts [42,43]. Finally, the devices were accomplished by evaporating Ca/Al electrodes with an area of 4.15 mm². All the fabrication processes except for the spin-coating of the PEDOT:PSS layers were carried out inside a nitrogen glovebox. To obtain reliable results, the current density-voltage (*J*-*V*) characteristics were measured under 100 mW cm⁻² standard AM 1.5 G spectrum by using a Class AAA solar simulator along with a NIM calibrated KG3-filtered reference cells according to our recent report [44].

Synthesis

2,3-Dioctylthiophene (2)

To a solution of 2-bromo-3-octylthiophene (30 mmol, 8.28 g) and $\text{Ni}(\text{dppp})\text{Cl}_2$ (0.36 mmol, 194 mg) in THF (50 mL), the Grignard reagent (2 M, 18 mL) was added dropwise at 0°C under the protection of argon. Then the reaction was stirred under reflux overnight. The mixture was quenched by diluted HCl slowly, washed by water and extracted by ethyl ether twice, then the combined organic layer was

concentrated by removing the solvent and the coarse product was purified by distillation, after which the pure compound 2 (4.1 g, yield 44%) was obtained as colorless liquid. ^1H NMR (CDCl_3 , 400 MHz), δ (ppm): 6.98(d, 1H), 6.78(d, 1H), 2.73 (t, 2H), 2.51 (t, 2H), 1.75–1.60 (m, 4H), 1.30 (m, 20H), 0.88 (t, 6H).

2-Bromo-5-octylthiophene (3)

In a three neck round flask, *N*-bromosuccinimide (NBS) (17.8 g, 0.1 mol) was added to a solution of 5-octylthiophene (19.6 g, 0.1 mol) in *N,N*-dimethylformamide (DMF) (150 mL) by portions at 0°C and the reaction was slowly warmed to room temperature for 2 h. Then the reaction was quenched by 100 mL of water and extracted by ethyl ether three times. After the solvent of organic phase was removed, the crude product was purified by distillation and compound 3 (24.3 g, yield 88%) was obtained. ^1H NMR (CDCl_3 , 400 MHz), δ (ppm): 6.84 (d, 1H), 6.53 (d, 1H), 2.74 (t, 2H), 1.65 (m, 2H), 1.31 (m, 10H), 0.89 (t, 3H).

3-Bromo-5-octylthiophene (4)

To a solution of compound 3 (5.52 g, 20 mmol) in THF (30 mL), lithium diisopropylamide (2 M, 13 mL) was added dropwise at -78°C under protection of argon, then the solution was warmed to room temperature slowly and kept for 16 h. After that the reaction was quenched by water slowly, and the mixture was extracted by ethyl ether twice. The organic phase was concentrated by removing the solvent and the raw product was purified by distillation to get pure compound 4 as a colorless liquid (5.30 g, yield 96%). ^1H NMR (CDCl_3 , 400 MHz), δ (ppm): 7.00 (s, 1H), 6.70 (s, 1H), 2.78 (t, 2H), 1.66 (m, 2H), 1.31 (m, 10H), 0.90 (t, 3H).

2,4-Dioctylthiophene (5)

The same method of synthesizing compound 2 was used to prepare compound 5 as a colorless liquid (yield 63%). ^1H NMR (CDCl_3 , 400 MHz), δ (ppm): 6.68 (s, 1H), 6.62 (s, 1H), 2.77 (t, 2H), 2.55 (t, 2H), 1.70–1.57 (m, 4H), 1.32 (m, 20H), 0.90 (t, 6H).

4,8-Bis(5-(2-hexyldecyl)thiophen-2-yl)benzo[1,2-*b*:4,5-*b'*]dithiophene (BDT-*o*)

To a solution of compound 2 (6.2 g, 20 mmol) in THF (20 mL), *n*-butyllithium (2.5 M, 8.8 mL) was added dropwise at 0°C under protection of argon, then the mixture was warmed to 50°C and stirred for 0.5 h. Subsequently, benzo[1,2-*b*:4,5-*b'*]dithiophene-4,8-dione (1.1 g, 5 mmol) was added and stirred for 1 h. A solution of $\text{SnCl}_2 \cdot 2\text{H}_2\text{O}$ (9.0 g, 40 mmol) in 10% HCL was added when the reactant came back to room temperature, then the reactant was stirred for another 2 h. The mixture was poured into ice water and extracted with diethyl ether three times, and the

organic phase was concentrated by removing the solvent. The coarse product was purified by silica gel chromatography using petroleum ether as eluent to get pure BDT-*o* (1.40 g, yield 35%). ¹H NMR (CDCl₃, 400 MHz), δ (ppm): 7.69 (d, 2H), 7.45 (d, 2H), 7.21 (s, 2H), 2.84 (t, 4H), 2.62 (t, 4H), 1.76–1.61 (m, 8H), 1.45–1.30 (m, 40H), 0.90–0.84 (m, 12H).

*4,8-Bis(2,4-dioctylthiophene-5-yl)benzo[1,2-b;4,5-b']dithiophene (BDT-*m*)*

Under the protection of argon, *n*-butyllithium (2.5 M, 8.8 mL) was added dropwise into a solution of compound 5 (6.20 g, 20 mmol) in THF (20 mL) at 0°C, then the mixture was warmed up to 50°C and stirred for 0.5 h. Subsequently, 4,8-dehydrobenzo[1,2-b;4,5-b']dithiophene-4,8-dione (1.1 g, 5 mmol) was added and the mixture was stirred for 1 h at 50°C. After cooling down to ambient temperature, a mixture of SnCl₂·2H₂O (9.0 g, 40 mmol) in 10% HCl was added and the mixture was stirred for additional 2 h. Then the mixture was poured into ice water, extracted by ethyl ether twice and the combined organic phase was concentrated to obtain raw compound BDT-*m*. Further purification was carried out by a chromatographic column using petroleum ether as eluent to obtain pure compound BDT-*m* as yellow stick liquid (1.84 g, yield 46%). ¹H NMR (CDCl₃, 400 MHz), δ (ppm): 7.39 (d, 2H), 7.24 (m, 2H), 6.78 (s, 2H), 2.88 (t, 4H), 2.36 (t, 4H), 1.77 (m, 8H), 1.36 (br, 40H), 0.91–0.79 (m, 12H).

2,6-Bis(trimethyltin)-4,8-bis(2,3-dioctylthiophene-5-yl)benzo[1,2-b;4,5-b']dithiophene (M2)

Under the protection of argon, *n*-butyllithium (2.5 M, 2.0 mL) was added dropwise into the solution of BDT-*o* (1.60 g, 2.0 mmol) in THF (30 mL) at room temperature and stirred for 2 h at 50°C. Then trimethyltin chloride (1.0 M, 6 mL) was added to the solution at room temperature. 2 h later, the reaction was quenched by water (80 mL) and extracted by ethyl ether twice. After removing the solvent, the crude compound M2 was purified by recrystallized to obtain pure compound M2 as light yellow powder (1.42 g, yield 63%). ¹H NMR (CDCl₃, 400 MHz), δ (ppm): 7.73 (s, 2H), 7.24 (s, 2H), 2.86 (t, 4H), 2.64 (t, 4H), 1.78–1.63 (m, 8H), 1.46–1.30 (br, 40H), 0.90 (m, 12H), 0.40 (m, 18H).

2,6-Bis(trimethyltin)-4,8-bis(2,4-dioctylthiophene-5-yl)benzo[1,2-b;4,5-b']dithiophene (M3)

n-Butyllithium (2.5 M, 2.08 mL) was added dropwise into the solution of BDT-*m* (1.60 g, 2.0 mmol) in THF (30 mL) at room temperature under the protection of argon, and the mixture stirred for 2 h at 50°C. Then trimethyltin chloride (1.0 M, 6 mL) was added to the solution at room temperature and stirred for 2 h. Then the reaction was quenched

by water (80 mL) and extracted by ethyl ether twice. After removing the solvent, the crude compound M3 was purified by recrystallized to obtain pure compound M3 (1.78 g, yield 79%). ¹H NMR (CDCl₃, 400 MHz), δ (ppm): 7.72 (s, 2H), 7.30 (s, 2H), 2.88 (t, 4H), 2.36 (t, 4H), 1.74 (m, 8H), 1.41–1.31 (br, 40H), 0.91–0.79 (m, 12H), 0.40 (s, 18H).

*Polymerization of PBDTDTBT-*p*, PBDTDTBT-*o*, PBDTDTBT-*m**

BDT monomer (0.5 mmol) and DTBT monomer (0.5 mmol) were put into a 50 mL two-neck flask, and 10 mL of toluene was added. The mixture was stirred and purged with argon for 5 minutes, and then 20 mg of catalyst Pd(PPh₃)₄ was added. After being purged for 20 minutes, the mixture was put into a 110°C oil bath. After 14 h, the reaction was quenched by adding 20 mL of methanol. The solid was filtered into a Soxhlet funnel and extracted by methanol, hexane, and chloroform successively. The chloroform fraction was collected, concentrated and precipitated from a large amount of methanol. The precipitants were filtered and dried under vacuum. The yield and elemental analytical data of the polymers are as follows.

PBDTDTBT-*p*: Yield 61%. Calculated for C₆₄H₇₈N₂S₇: C, 69.89; H, 7.15; N, 2.55; S, 20.41; Found: C, 69.77; H, 7.14; N, 2.49. M_n = 28 k Da; PDI = 1.9.

PBDTDTBT-*o*: Yield 58%. Calculated for C₆₄H₇₈N₂S₇: C, 69.89; H, 7.15; N, 2.55; S, 20.41; Found: C, 69.87; H, 7.11; N, 2.52. M_n = 25 k Da; PDI = 1.7.

PBDTDTBT-*m*: Yield 37%. Calculated for C₆₄H₇₈N₂S₇: C, 69.89; H, 7.15; N, 2.55; S, 20.41; Found: C, 69.85; H, 7.14; N, 2.55. M_n = 18 k Da; PDI = 1.8.

Received 24 January, 2015; accepted 13 February, 2015

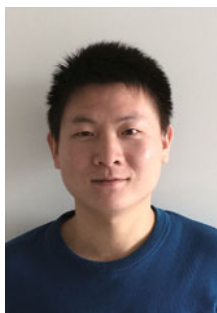
- Dou L, You J, Hong Z, *et al.* 25th anniversary article: a decade of organic/polymeric photovoltaic research. *Adv Mater*, 2013, 25: 6642–6671
- Cheng YJ, Yang SH, Hsu CS. Synthesis of conjugated polymers for organic solar cell applications. *Chem Rev* 2009, 109: 5868–5923
- Chen J, Cao Y. Development of novel conjugated donor polymers for high-efficiency bulk-heterojunction photovoltaic devices. *Acc Chem Res*, 2009, 42: 1709–1718
- Beaujuge PM, Fréchet JMJ. Molecular design and ordering effects in π -functional materials for transistor and solar cell applications. *J Am Chem Soc*, 2011, 133: 20009–20029
- Li YF. Molecular design of photovoltaic materials for polymer solar cells: toward suitable electronic energy levels and broad absorption. *Acc Chem Res*, 2012, 45: 723–733
- Zhou HX, Yang LQ, You W. Rational design of high performance conjugated polymers for organic solar cells. *Macromolecules*, 2012, 45: 607–632
- Duan C, Huang F, Cao Y. Recent development of push-pull conjugated polymers for bulk-heterojunction photovoltaics: rational design and fine tailoring of molecular structures. *J Mater Chem*, 2012, 22: 10416–10434
- Ye L, Zhang S, Huo L, Zhang M, Hou J. Molecular design toward

- highly efficient photovoltaic polymers based on two-dimensional conjugated benzodithiophene. *Acc Chem Res*, 2014, 47: 1595–1603
- 9 Huo LJ, Hou JH. Benzo[1,2-b:4,5-b']dithiophene-based conjugated polymers: band gap and energy level control and their application in polymer solar cells. *Polym Chem*, 2011, 2: 2453–2461
- 10 You J, Dou L, Yoshimura K, *et al.* A polymer tandem solar cell with 10.6% power conversion efficiency. *Nat Commun*, 2013, 4: 1446
- 11 Tan Z, Li S, Wang F, *et al.* High performance polymer solar cells with as-prepared zirconium acetylacetonate film as cathode buffer layer. *Sci Rep*, 2014, 4: 4691
- 12 Ye L, Zhang SQ, Ma W, *et al.* From binary to ternary solvent: morphology fine-tuning of D/A blends in PDPP3T-based polymer solar cells. *Adv Mater*, 2012, 24: 6335–6341
- 13 Li W, Furlan A, Hendriks KH, Wienk MM, Janssen RAJ. Efficient tandem and triple-junction polymer solar cells. *J Am Chem Soc*, 2013, 135: 5529–5532
- 14 Li K, Li Z, Feng K, *et al.* Development of large band-gap conjugated copolymers for efficient regular single and tandem organic solar cells. *J Am Chem Soc*, 2013, 135: 13549–13557
- 15 He ZC, Zhong CM, Su SJ, *et al.* Enhanced power-conversion efficiency in polymer solar cells using an inverted device structure. *Nat Photonics*, 2012, 6: 591–595
- 16 Chen CC, Chang WH, Yoshimura K, *et al.* An efficient triple-junction polymer solar cell having a power conversion efficiency exceeding 11%. *Adv Mater*, 2014, 26: 5670–5677
- 17 Li XH, Choy WCH, Huo LJ, *et al.* Dual plasmonic nanostructures for high performance inverted organic solar cells. *Adv Mater*, 2012, 24: 3046–3052
- 18 Yang TB, Wang M, Duan CH, *et al.* Inverted polymer solar cells with 8.4% efficiency by conjugated polyelectrolyte. *Energ Environ Sci*, 2012, 5: 8208–8214
- 19 Liu S, Zhang K, Lu J, *et al.* High-efficiency polymer solar cells via the incorporation of an amino-functionalized conjugated metallo-polymer as a cathode interlayer. *J Am Chem Soc*, 2013, 135: 15326–15329
- 20 Liao SH, Jhuo HJ, Cheng YS, Chen SA. Fullerene derivative-doped zinc oxide nanofilm as the cathode of inverted polymer solar cells with low-bandgap polymer (PTB7-Th) for high performance. *Adv Mater*, 2013, 25: 4766–4771
- 21 Li CZ, Chang CY, Zang Y, *et al.* Suppressed charge recombination in inverted organic photovoltaics via enhanced charge extraction by using a conductive fullerene electron transport layer. *Adv Mater*, 2014, 26: 6262–6267
- 22 Zhang S, Ye L, Zhao W, *et al.* Side chain selection for designing highly efficient photovoltaic polymers with 2D-conjugated structure. *Macromolecules*, 2014, 47: 4653–4659
- 23 Zhou H, Zhang Y, Mai CK, *et al.* Conductive conjugated polyelectrolyte as hole-transporting layer for organic bulk heterojunction solar cells. *Adv Mater*, 2014, 26: 780–785
- 24 Liu P, Zhang K, Liu F, *et al.* Effect of fluorine content in thienothiophene-benzodithiophene copolymers on the morphology and performance of polymer solar cells. *Chem Mater*, 2014, 26: 3009–3017
- 25 Ye L, Zhang S, Zhao W, Yao H, Hou J. Highly efficient 2D-conjugated benzodithiophene-based photovoltaic polymer with linear alkylthio side chain. *Chem Mater*, 2014, 26: 3603–3605
- 26 Cui C, Wong WY, Li Y. Improvement of open-circuit voltage and photovoltaic properties of 2D-conjugated polymers by alkylthio substitution. *Energ Environ Sci*, 2014, 7: 2276–2284
- 27 Tan ZA, Li LJ, Wang FZ, *et al.* Solution-processed rhenium oxide: a versatile anode buffer layer for high performance polymer solar cells with enhanced light harvest. *Adv Energy Mater*, 2014, 4: 1300884
- 28 Zhao W, Ye L, Zhang S, *et al.* Ultrathin polyaniline-based buffer layer for highly efficient polymer solar cells with wide applicability. *Sci Rep*, 2014, 4: 6570
- 29 Zhang M, Gu Y, Guo X, *et al.* Efficient polymer solar cells based on benzothiadiazole and alkylphenyl substituted benzodithiophene with a power conversion efficiency over 8%. *Adv Mater*, 2013, 25: 4944–4949
- 30 Wang N, Chen Z, Wei W, Jiang Z. Fluorinated benzothiadiazole-based conjugated polymers for high-performance polymer solar cells without any processing additives or post-treatments. *J Am Chem Soc*, 2013, 135: 17060–17068
- 31 Cabanetos C, El Labban A, Bartelt JA, *et al.* Linear side chains in benzo[1,2-b:4,5-b']dithiophene-thieno[3,4-c]pyrrole-4,6-dione polymers direct self-assembly and solar cell performance. *J Am Chem Soc*, 2013, 135: 4656–4659
- 32 Lei T, Wang JY, Pei J. Roles of flexible chains in organic semiconducting materials. *Chem Mater*, 2013, 26: 594–603
- 33 Mei J, Bao Z. Side chain engineering in solution-processable conjugated polymers. *Chem Mater*, 2013, 26: 604–615
- 34 Zhang ZG, Li YF. Side-chain engineering of high-efficiency conjugated polymer photovoltaic materials. *Sci China Chem*, 2015, 58: 192–209
- 35 Huang Y, Zhang M, Ye L, *et al.* Molecular energy level modulation by changing the position of electron-donating side groups. *J Mater Chem*, 2012, 22: 5700–5705
- 36 Huang F, Chen KS, Yip HL, *et al.* Development of new conjugated polymers with donor- π -bridge-acceptor side chains for high performance solar cells. *J Am Chem Soc*, 2009, 131: 13886–13887
- 37 Dong Y, Hu X, Duan C, *et al.* A series of new medium-bandgap conjugated polymers based on naphtho[1,2-c:5,6-c']bis(2-octyl-[1,2,3]triazole) for high-performance polymer solar cells. *Adv Mater*, 2013, 25: 3683–3688
- 38 Huo LJ, Hou JH, Zhang SQ, Chen HY, Yang Y. A polybenzo[1,2-b:4,5-b']dithiophene derivative with deep HOMO level and its application in high-performance polymer solar cells. *Angew Chem Int Ed*, 2010, 49: 1500–1503
- 39 Peng Q, Liu X, Su D, *et al.* Novel benzo[1,2-b:4,5-b']dithiophenbenzothiadiazole derivatives with variable side chains for high-performance solar cells. *Adv Mater*, 2011, 23: 4554–4558
- 40 Frisch MJ, Trucks GW, Schlegel HB, *et al.* Gaussian 09. Wallingford: Gaussian, Inc.; 2009
- 41 Huo L, Guo X, Zhang S, Li Y, Hou J. PBDTTTz: a broad band gap conjugated polymer with high photovoltaic performance in polymer solar cells. *Macromolecules*, 2011, 44: 4035–4037
- 42 Ye L, Jing Y, Guo X, *et al.* Remove the residual additives toward enhanced efficiency with higher reproducibility in polymer solar cells. *J Phys Chem C*, 2013, 117: 14920–14928
- 43 Wang Y, Liu Y, Chen S, Peng R, Ge Z. Significant enhancement of polymer solar cell performance via side-chain engineering and simple solvent treatment. *Chem Mater*, 2013, 25: 3196–3204
- 44 Ye L, Zhou C, Meng H, *et al.* Toward reliable and accurate evaluation of polymer solar cells based on low band gap polymers. *J Mater Chem C*, 2015, 3: 564–569

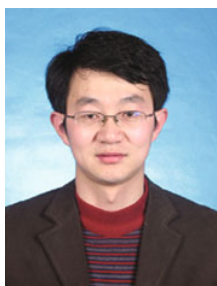
Acknowledgements This work was supported by the National Basic Research Program 973 (2014CB643500), the National Natural Science Foundation of China (91333204 and 51261160496), and the Chinese Academy of Sciences (XDB12030200 and KJZDEW-J01).

Author contributions Hou J and Huo L designed this work. Yao H synthesized the materials and wrote the paper. Ye L and Fan B conducted the other experiments. All authors contributed to discuss the results.

Conflict of interest The authors declare that they have no conflict of interest.



Huifeng Yao is a PhD candidate at the Institute of Chemistry, Chinese Academy of Sciences (ICCAS) under the supervision of Prof. Jianhui Hou. His research interests focus on the design and synthesis of high performance organic photovoltaic materials.



Lijun Huo received his PhD from China University of Mining and Technology in 2010. He was an associate professor in Prof. Jianhui Hou's group at ICCAS, and then joined Beihang University in 2014. His current research interests are the design and synthesis of organic photovoltaic materials.



Jianhui Hou received his PhD from ICCAS in 2006. Then he worked as postdoctoral researcher in Prof. Yang Yang's group at University of California at Los Angeles. He joined the Solarmer Energy Inc. (USA) in 2008 as a team leader of research department. He became a full professor at ICCAS since 2010, and his research focuses on the design, synthesis and application of the organic/polymer photovoltaic materials. In the past few years, he has co-authored >100 papers in peer-reviewed journals and 18 patents.

中文摘要 本文将具有不同取代位点的二维共轭支链引入到PBDTDTBT类聚合物的苯并二噻吩单元上, 设计和合成了三种骨架相同的二维共轭聚合物, 即PBDTDTBT-*p*, PBDTDTBT-*o*和PBDTDTBT-*m*, 并在此基础上探究了烷基链取代位点对共轭聚合物的光伏性质以及器件性能的影响. 通过吸收光谱、循环伏安、热失重分析、X射线衍射、光伏测试以及理论计算等手段对比研究了三种聚合物光伏材料, 结果表明由不同烷基链取代位点引起的分子空间位阻作用对三种聚合物的光物理性质、微观形貌以及光伏性能有着重要的影响. 基于三种聚合物制备的光伏器件的开路电压可从0.67 V变化到0.90 V, 其光伏效率也相应地从3.48%提高到5%以上. 调节烷基链取代位点是一种简单有效制备高性能聚合物光伏材料的优化策略.